INT. J. GEOGRAPHICAL INFORMATION SCIENCE
VOL. 18, NO. 6, SEPTEMBER 2004, 595–609

Taylor & Francis
Taylor & Francis Group

Research Article

Effect of support size on the accuracy of a distributed rockfall model

L. K. A. DORREN
Cemagref Grenoble, 2 rue de la Papeterie, B.P. 76, F-38402 St. Martin d'Hères cedex, France; e-mail: luuk.dorren@cemagref.fr
IBED, Universiteit van Amsterdam, Amsterdam, The Netherlands

G. B. M. HEUVELINK
Laboratory of Soil Science and Geology, Wageningen University, PO Box 37, NL-6700 AA Wageningen, The Netherlands; e-mail: gerard.heuvelink@wur.nl

(*Received 3 January 2003; accepted 26 August 2003*)

Abstract. It is investigated whether a GIS-based distributed model developed for rockfall assessment at slope scale, which uses data with a support of 2.5×2.5 m, could be used for rockfall assessment at the regional scale, using input data with a support of 25×25 m and of poorer quality. It was anticipated that in the latter case the model error would increase. Three types of simulations were applied to the same model and the outcomes were validated with field data. The first simulation used input data with a support of 2.5×2.5 m and aggregated the output to a support of 25×25 m. The second simulation used the same input data as in the first simulation, but these data were aggregated to a support of 25×25 m before running the model. The third simulation used input data of poorer quality obtained at a support of 25×25 m. The results show that simulating the maximum extent of rockfall runout zones with a distributed model using data with a support of 25×25 m is realistic and feasible. This is also true for data with poorer quality as the third simulation resulted in a slightly larger mean-squared error than the first simulation. Surprisingly, it also gave a smaller error than the second simulation. We investigated the cause of the large error produced by the second simulation and concluded that this was mainly caused by the combination of a high-quality digital elevation model and the loss of spatial structure in the input data due to spatial aggregation.

1. Introduction

Geomorphological research focuses on understanding processes, patterns and landforms in geoecosystems. This type of research contributes to the basis needed for identifying, assessing and perhaps solving or preventing environmental problems such as soil erosion, flooding and rapid mass movements. Distributed models are increasingly popular tools within geomorphological research (Willgoose *et al.* 1991, Montgomery and Dietrich 1994, Tucker *et al.* 2001). They provide excellent frameworks for the conceptualization of developed theories and for simulating current or future processes and patterns in geoecosystems.

Models are simplified representations of reality and therefore model outcomes

International Journal of Geographical Information Science
ISSN 1365-8816 print/ISSN 1362-3087 online © 2004 Taylor & Francis Ltd
http://www.tandf.co.uk/journals
DOI: 10.1080/13658810410001703804

always deviate from 'the truth' to some extent and contain errors or uncertainties. These are caused partly by the model's simplification of the reality, but also because model input data are rarely known exactly and also probably contain errors (Burrough and McDonnell 1998). The degree of model simplification depends on the availability and quality of input data, which are often determined by the feasibility of measuring the inputs with sufficient detail. Clearly, it is more difficult to obtain detailed input data for a large catchment than for a small monitoring plot. Therefore, models and their input and output data are usually less detailed when moving up from a smaller to a larger spatial scale (Heuvelink 1998). Uncertainties or errors of model outcomes are thus related to spatial scale, of which one factor is the 'support' of the model input data. Here, support is defined as the largest area treated as homogenous such that an average value of the property of interest is known but not the variation within (Bierkens *et al.* 2000). Errors of model outcomes do not necessarily increase at larger supports. For example, aggregating data to large supports could decrease uncertainties about the average value in a large raster cell (Van Rompaey *et al.* 1999). On the other hand, if the model input data have a large support, errors in the model outcomes could increase due to the loss of terrain information. The input data for a model should be of sufficient detail to capture the spatial variation that is essential to describe the process or pattern being modelled (Goodchild 2001). In most cases a simpler or at least another model structure is required for modelling larger study areas, since the processes controlling changes in spatial patterns are different at different spatial scales (Bergkamp 1995). In some cases, however, the same model can be used for both a small and a large spatial scale, only the support of the input data may change.

The present paper focuses on a GIS-based distributed model developed for rockfall assessment at the slope scale, which was designed to use input data with a support of 2.5×2.5 m. The main objective was to analyse whether such a model could also be used for a larger scale (e.g. regional scale, for a study area covering 500 km^2), using input data on a support of 25×25 m. The larger support data are of poorer quality because they have less detail and involve a reduced sampling or mapping effort. It was anticipated that the model using data with a support of 25×25 m would produce a larger error than that used on a support of 2.5×2.5 m. The hypothesis was that poor data quality is the main cause of a larger model prediction error rather than the effect of simulating a similar process on a larger support. The distributed rockfall model was applied with data on a support of 2.5×2.5 m. Subsequently, the same model was applied using the same data aggregated to a support of 25×25 m. Finally, the model was applied using input data of poorer quality, which were obtained directly at a support of 25×25 m. The main objective is to determine how realistic or feasible rockfall simulation is with data on a support of 25×25 m.

2. Method and model overview

Three simulation schemes were defined to analyse the effect of input data with different aggregation levels on the accuracy of the output (figure 1). In simulation scheme 1, input data with a support of 2.5×2.5 m were used. The output was aggregated to a support of 25×25 m by averaging the outputs on the 2.5×2.5 m support. The output data were compared with validation data at the same support.

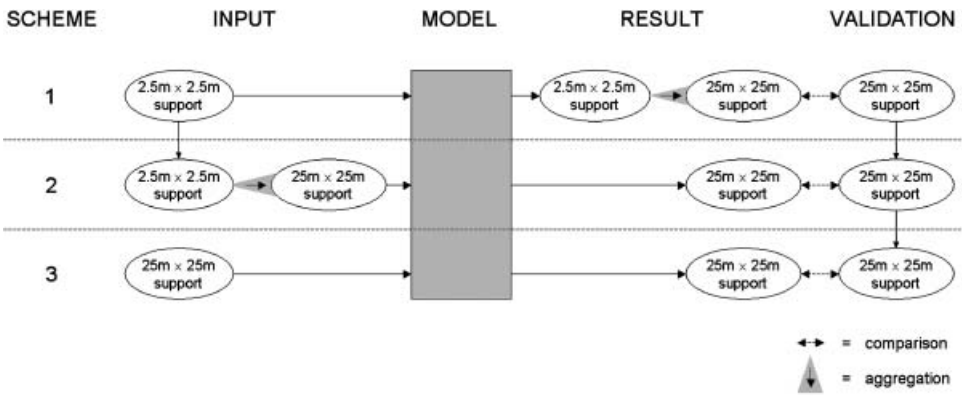

Figure 1. Three simulation schemes tested. For explanations, see the text.

In simulation scheme 2, the same input data were used as before but they were aggregated to a support of 25×25 m before running the rockfall model. In simulation scheme 3, the support of data was the same as in scheme 2, but the input data for simulation scheme 3 were obtained directly at a support of 25×25 m. Since the data used in simulation scheme 3 were obtained at the regional scale and thus less detailed than the data used in simulation schemes 1 and 2, it can be stated that the quality of these data was considerably poorer.

The same rockfall simulation model was used throughout the three simulation schemes. This model simulates a falling rock by calculating the kinetic energy balance during sequences of motion though the air and collisions on the slope surface or against trees. Start locations for the rockfall simulations were derived from field mapped rockfall source areas. From each start location, one single falling rock was simulated. For details of the used rockfall simulation program, see Dorren *et al.* (2004). A sensitivity test of the model showed that repeating the simulations 100 times using the Monte Carlo method (Lewis and Orav 1989, Mowrer 1997) produced sufficiently stable results. This number of repetitions was considered an acceptable trade off between computation time and the stability of the obtained results.

Standard algorithms for a uniform accelerated parabolic movement through the air calculated the motions through the air. Algorithms modified from Pfeiffer and Bowen (1989) calculated the energy balance before and after collisions with the slope surface and tree stems. The modifications were such that the factor compensating for the effect of the rockfall velocity on the elasticity of the collision was left out, because the empirical constants required to calculate it were not available for the study site. The algorithms for bouncing and motion through the air were combined with a procedure that calculated the fall direction based on a digital elevation model (DEM) as described in Section 3. A flow diagram of the model is given in figure 2.

The model inputs that are affected by a change of support, which were also the model inputs focused on in this study, are a DEM, the rasters containing values for the tangential and normal coefficient of restitution and the tree distribution raster, which includes both the number of trees per cell and the range of tree stem diameters. The DEM was used to determine the mean slope gradient and therefore the acceleration and deceleration of a falling block. Furthermore, the DEM

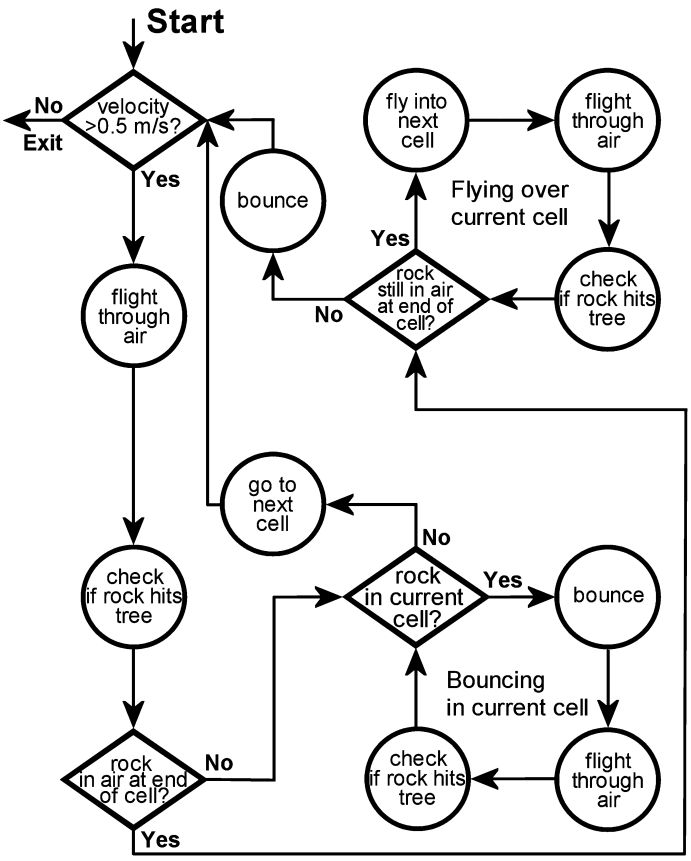

Figure 2. Flow diagram of the model used in the three simulation schemes.

determined the fall direction. The coefficients of restitution determined the amount of energy lost during a bounce, where the tangential coefficient of restitution determines energy loss parallel to the slope surface (due to surface roughness or vegetation) and the normal coefficient of restitution determines energy loss perpendicular to the slope surface (due to elasticity of the material covering the slope surface). The tree distribution determined the probability of a falling rock hitting a tree.

The outcomes produced by the three simulation schemes were compared with a validation data set on the basis of the mean error (ME) and the mean-squared error (MSE) following:

$$ME = \frac{1}{n}\sum_{i=1}^{n}(P_i - O_i) \tag{1}$$

$$MSE = \frac{1}{n}\sum_{i=1}^{n}(P_i - O_i)^2, \tag{2}$$

where n is the number of observations, P_i is the modelled or predicted value in raster cell i, and O_i is the observed value in raster cell i, which is obtained from the

validation data. The correlation coefficients between the observed and predicted values were also calculated for each simulation scheme.

3. Test site and available data

The test site was a forested, active rockfall slope in the most western part of the Austrian Alps, located at 47°00′ latitude and 10°01′ longitude. The site could be divided into two areas. The rockfall source area, which is a steep cliff face dissected by large denudation niches and an accumulation area, and a large post-glacially developed talus cone consisting mainly of rockfall scree, but also some debris flow material. The mean slope gradient in the source area was approximately 70° and in the accumulation area 38°, The slope length of the talus cone is approximately 900 m. An overview of the site is shown in figure 3.

Two DEMs were available for the site, both raster based with supports of 25×25 m (LRDEM) and 2.5×2.5 m (HRDEM). The LRDEM was created by interpolation of photogrammetric height measurements at a ground distance of 50 m, enhanced and supplemented with prominent terrain structures. The given maximum error in this DEM was 20 m (BEV 2002).

The HRDEM was derived from a TIN (Triangular Irregular Network), which was created from contour lines with an equidistance of 5 m. The contour lines were derived from a combined data set consisting of slope transects measured in the field, a detailed geomorphological field map (1:2000) and existing contour lines with an equidistance of 20 m. Since the site was fully covered with forest, we did not use a tachymeter or photogrammetric height measurements based on aerial photographs

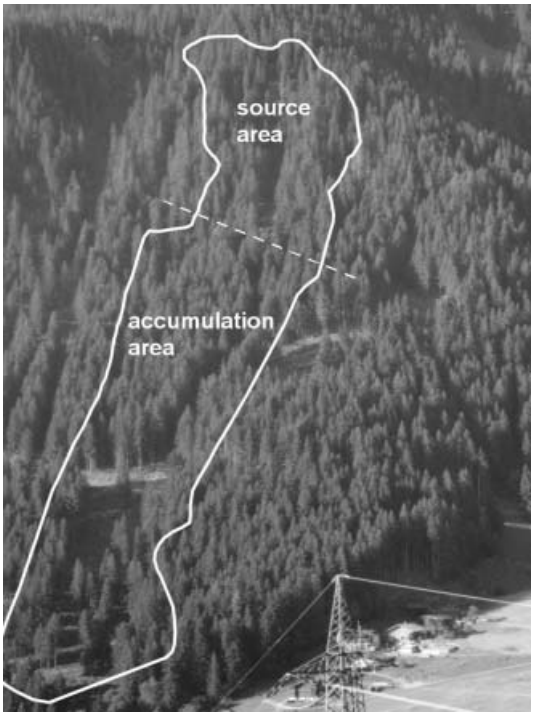

Figure 3. Part of the 'Ausserbacher' forest in the Montafon region, Austria, that served as a test site for the study. The white outline represents the test site.

to create the HRDEM. The maximum error of the HRDEM was 6 m. The main difference between the HRDEM and the LRDEM was that important terrain structures, which determine the variation in the slope gradient of the site, were well represented in the HRDEM, whereas in the LRDEM such structures were not evident at all (figure 4).

Maps of mean slope gradients were derived from both the HRDEM and the LRDEM using the method described by Zevenbergen and Thorne (1987). In addition, fall directions were calculated using a modified multiple-flow algorithm (Quinn *et al*. 1991, Wolock and McGabe 1995, Tarboton 1997). To randomize the fall direction from a central cell for each simulation run, this method calculated a fall direction raster map by sampling the fall direction for each cell randomly from a probability distribution. The latter was determined by the steepness of the mean slope gradients between the central cell and all its downslope neighbouring cells.

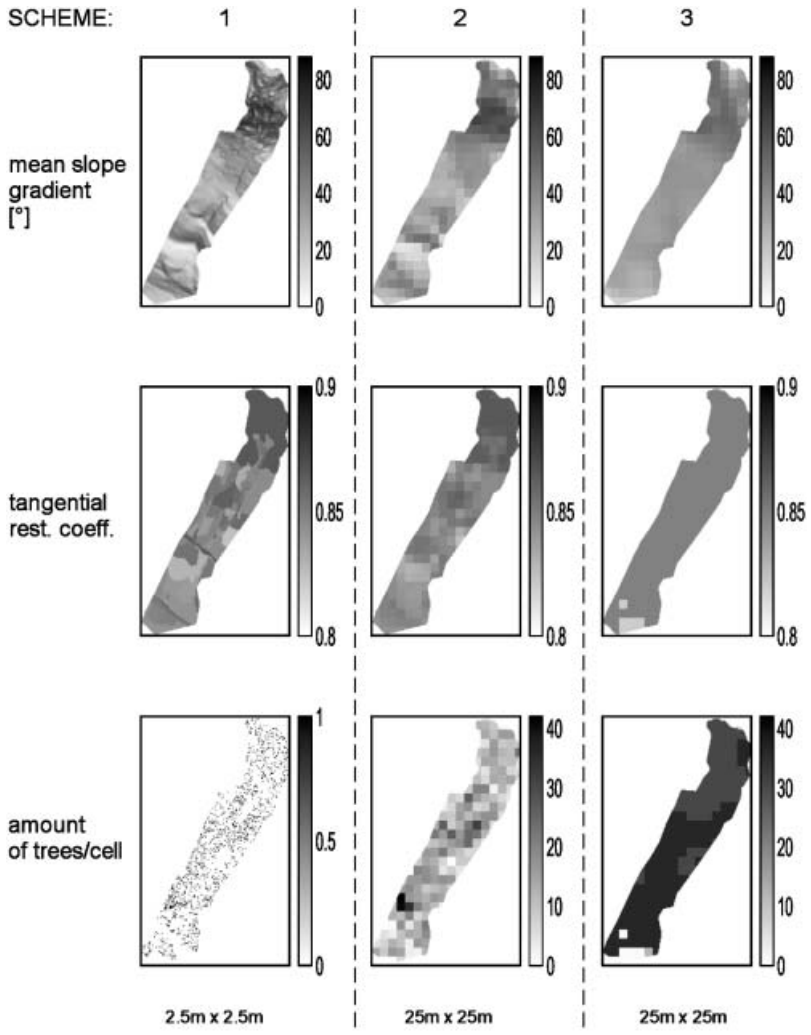

Figure 4. Slope, tangential coefficient of restitution (r_t) and number of trees per cell for simulation schemes 1–3.

The probability of a rock falling to a downslope cell was largest towards the lowest downslope cell. For details about the procedure used, see Dorren *et al.* (2004).

The tangential coefficient of restitution (r_t), the normal coefficient of restitution (r_n) and the tree distribution were represented as raster maps with a support of 25×25 m (hereafter, respectively, LRr_t, LRr_n and LRtree) and with a support of 2.5×2.5 m (hereafter HRr_t, HRr_n and HRtree). The coefficients of restitution determine the energy efficiency of a collision (Chau *et al.* 2002). The vegetation cover and the surface roughness determine the tangential coefficient of restitution. The normal coefficient of restitution is determined by the elasticity of the slope surface. The LRr_t and LRr_n were derived from data from the literature (Pfeiffer and Bowen 1989, Kobayashi *et al.* 1990, Van Dijke and Van Westen 1990, Giani 1992, Azzoni *et al.* 1995, Chau *et al.* 1998, Meißl 1998) and a land cover map, which was obtained by classifying a Landsat TM image of September 1998 (Dorren and Seijmonsbergen 2003). LRtree was also derived from this land cover map in combination with data from a regional forest inventory (Maier 1993). Both HRr_t and HRr_n were based on a detailed map (scale 1:2000) that depicted the spatial distribution of different hill-slope characteristics potentially affecting rockfall tracks (Dorren *et al.* 2004). From this map, r_t and r_n could be estimated using data from the literature (Pfeiffer and Bowen 1989, Van Dijke and Van Westen 1990, Kobayashi *et al.* 1990, Giani 1992, Azzoni *et al.* 1995, Chau *et al.* 1998, Meißl 1998). We created HRtree using a combination of a tree crown map and forest inventory data. The tree crown map was derived from an object-based classification of high-resolution digital colour-infrared (CIR) orthophotos (0.25×0.25 m) on which each individual tree crown was visible. The forest inventory, which was done with the 'Winkelzählprobe' method (Bitterlich 1948), provided additional data on the forest stands throughout the study site. This inventory method is also known as prism plot sampling or probability proportional to size sampling, i.e. the probability of a tree being selected within a sampling plot is proportional to the diameter of the tree (Shiver and Borders 1995). A grid was defined over the test site and tree stem diameters, the number of trees per ha and the rockfall damage per tree stem (number of fresh scars) were measured. From this inventory the tree volume, the number of trees and the damage per hectare were calculated for each grid cell.

HRDEM, HRr_t, HRr_n and HRtree were the input for simulation scheme 1. These data were aggregated for simulation scheme 2. LRDEM, LRr_t, LRr_n and LRtree provided input data for simulation scheme 3. A summation of all the values of the aggregated cells gave the aggregated tree map for simulation scheme 2. The input data for the three simulation schemes are given in table 1 and a flow diagram of the method is given in figure 4.

Validation data were extracted from the detailed forest inventory data. Within the grid cells covered by the forest inventory in the upper part of the accumulation area 18 squares of 25×25 m were selected randomly. We discarded the forest inventory data in the lower parts of the accumulation area because rockfall activity also originated from source areas outside the area used for this study. The size of the validation dataset is small ($n = 18$). Therefore results have to be interpreted carefully, though, these data are derived from a very large set of detailed measurements.

For these 18 squares, the tree volume and number of scars per hectare caused by

Table 1. Input data for the three simulation schemes and their origin.

Simulation scheme	Support	DEM	Tree distribution	r_t	r_n
1	2.5 × 2.5 m, HR	contour lines	orthophotos + detailed inventory	detailed field map + literature	detailed field map + literature
2	25 × 25 m, HR*	aggregated from 1	aggregated from 1	aggregated from 1	aggregated from 1
3	25 × 25 m, LR	photogrammetry	Landsat TM + regional inventory	Landsat TM + literature	Landsat TM + literature

HR, high resolution, large support; HR*, HR data aggregated to a 25 × 25 m support; LR, low resolution, small support.

rock impacts were measured. These data were compared with the number of rock impacts on trees as simulated by the model. For standardization purposes, both the validation data (observed values) and the simulated data (predicted values) in the 18 squares were expressed as percentages of the summed values of all the randomly selected squares. In other words, the observed value is the number of scars per unit tree volume in a square expressed as a percentage of the total number of scars per unit tree volume in all squares. Here, the number of scars per unit tree volume is the number of scars per hectare caused by rock impacts divided by the tree volume within the square. The predicted value represented the number of impacts in a square expressed as a percentage of the summed number of impacts in all squares.

4. Output of the three simulation schemes

Figure 5 shows the percentage of impacts in each cell for the three simulation schemes. They show a similar gradient in the number of impacts per cell. Most impacts occur in the upper right part of the area on the transition between the source area and the accumulation area. Generally, the number of impacts decreases towards the lower left, which is the accumulation area or runout zone. A notable

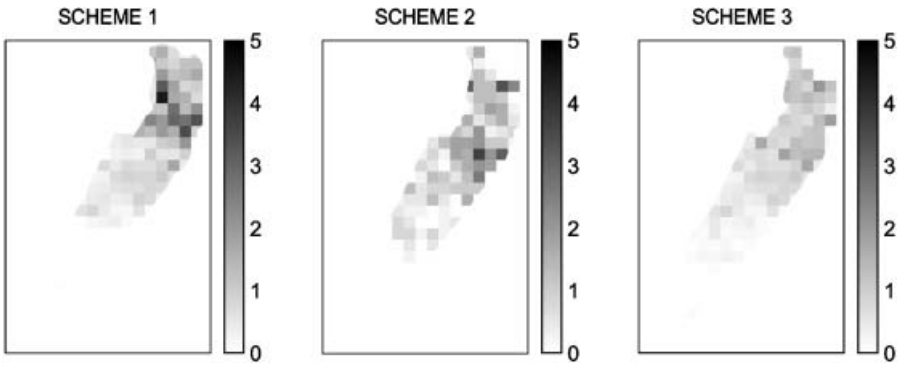

Figure 5. Produced relative numbers of impacts in a cell in percentages produced by simulation schemes 1–3.

difference between the three simulations is the location of the maximum number of impacts (figure 5). For simulation scheme 1, this is in the lower parts of the rockfall source areas, but for simulation schemes 2 and 3, it is located on the upper part of the accumulation area. However, for simulation scheme 3 the maximum number of impacts is more evenly distributed over the accumulation area.

Comparison of the simulated impacts with the number of observed scars per unit tree volume provided the results shown in figure 6. The histograms show that simulation scheme 2 produced the largest errors and simulation scheme 1 the smallest errors. In general, all errors are quite large. The scatter plots in figure 6 show the difference between each predicted and observed value for the three schemes in detail. The scatter plot of simulation scheme 1 shows that the degree of scatter between observed and predicted values is generally less than in the scatter plots of schemes 2 and 3. This is caused by a more accurate estimation of the larger observed values. Nevertheless, simulation scheme 1 also produced some considerable mismatches of the smaller observed values. The latter affects the mean-squared error considerably for simulation scheme 1 (MSE1), as shown in table 1 (MSE1 = 24.9). Simulation scheme 2 produced the largest error (MSE3 = 44.4) and simulation scheme 3 produced an intermediate one (MSE2 = 31.3). This is also indicated by the correlation coefficient (table 2). The correlation coefficient measures the strength of a linear relationship, but is not bound to the 1:1 relationship between observed and predicted values. The correlation coefficient is given here because it will indicate a systematic error in the model if both it and the MSE are large.

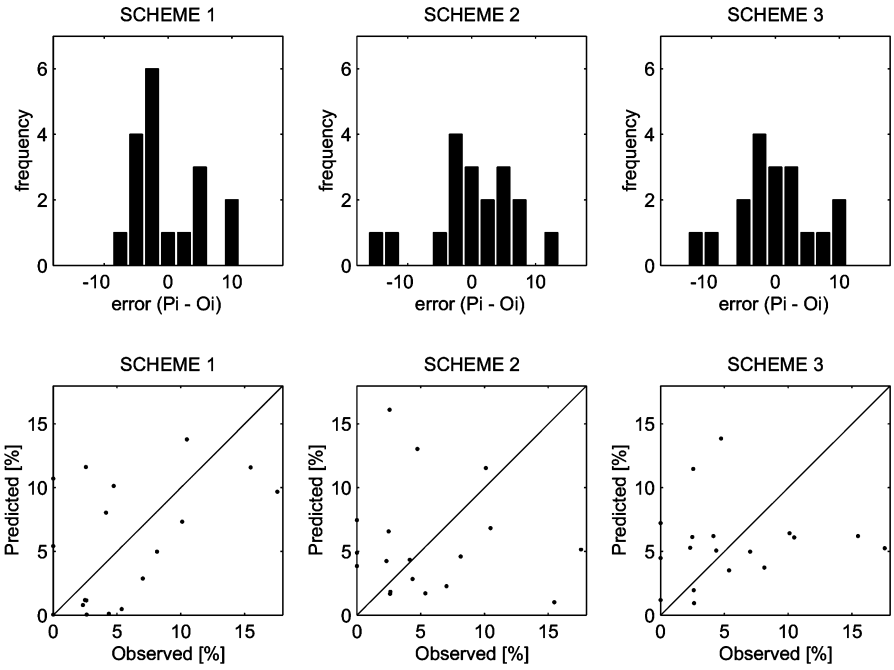

Figure 6. Histograms of the errors produced by simulation schemes 1–3 and accompanying scatter plots with observed versus predicted values.

Table 2. Mean error (ME), mean-squared error (MSE) and correlation coefficient (r) of the output of the three simulation schemes.

Simulation scheme	ME	MSE	r
1	0	24.9	0.47
2	0	44.4	0.08
3	0	31.3	0.09

5. Additional tests and discussion

5.1. *'Intermediate' simulation schemes*

We did not expect simulation scheme 3 to give a smaller MSE than scheme 2. Rather, we anticipated that scheme 3 would perform the worst, because it uses input data of the poorest quality. The only difference between simulation schemes 2 and 3 is the values for four model parameters, which have all been changed simultaneously. To assess which of these four input parameters caused a smaller MSE for simulation scheme 3, we analysed 'intermediate' simulation schemes. These 'intermediate' simulation schemes are explained in table 3.

The results presented in table 3 show that the substitution of LRtree by the aggregated HRtree (simulation scheme 7) resulted in an MSE of 29.3, which is smaller than the initial MSE for scheme 3 (figure 7a). Substitution of LRr_t by the

Table 3. Mean-squared error (MSE) of the model output produced with 'intermediate' simulation schemes 4–7 and the original schemes 2 and 3.

Simulation scheme	Used data	MSE
2	HRtree*, HRr_n*, HRr_t*, HRDEM*	44.4
3	LRtree, LRr_n, LRr_t, LRDEM	31.3
4	LRtree, LRr_n, LRr_t, HRDEM*	47.8
5	LRtree, LRr_n, HRr_t*, LRDEM	35.7
6	LRtree, HRr_n*, LRr_t, LRDEM	31.4
7	HRtree*, LRr_n, LRr_t, LRDEM	29.3

*Data aggregated to a 25×25 m support.

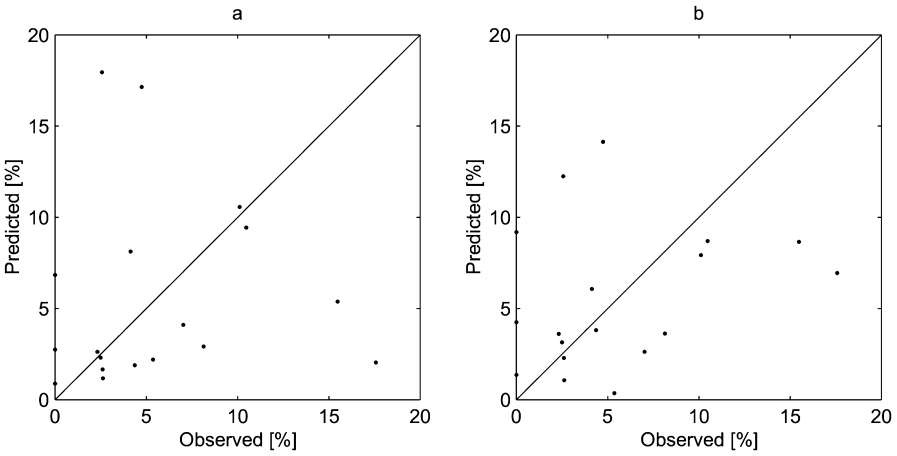

Figure 7. Scatter plots of (a) simulation scheme 7 and (b) simulation scheme 4.

aggregated HRr_t (simulation scheme 5) increased the MSE from 31.3 to 35.7. Table 2 also shows that the substitution of LRr_n by the aggregated HRr_n (simulation scheme 6) resulted in an increase of the MSE of 0.1, which indicates that the net effect of r_n on the simulation results was small.

A remarkable result is that the substitution of the LRDEM by the aggregated HRDEM (simulation scheme 4) did not decrease MSE3. On the contrary, it resulted in a large increase of the MSE from 31.3 to 47.8. The scatter plot of this simulation result is shown in figure 7b. This simulation scheme strongly overestimated the smaller observed values and strongly underestimated the larger observed values.

5.2. *Causes of simulation errors*

The 'intermediate' simulation scheme 4 indicated that the aggregated HRDEM was mainly responsible for the increase in error (table 2), which could be explained as follows. The transport channel shown in figure 3, which is represented in both the HRDEM and HRtree (figure 4), is averaged out to a certain extent in the aggregated HRDEM but still represented. Consequently, the fall directions calculated based on the aggregated HRDEM were generally towards this channel. This led to a concentration of falling rocks in the right side of the raster. Therefore, the number of impacts is more on that side of the area (figure 8; simulation scheme 4). This effect is reinforced by the fact that the transport channel is almost free of trees. Therefore, hardly any rock impacts against trees occur in the channel in reality. However, when using the aggregated HRtree, the forest structure in the channel as observed in the field and in HRtree is completely lost (figure 4). Consequently, the number of trees in the fall track of the simulated rocks, as represented by the aggregated HRtree, is overestimated, although the number of trees in the channel is still smaller than in the surrounding areas. As a result, the number of impacts in the channel is more strongly overestimated than in the other simulation schemes, as shown in figure 8 (simulation scheme 1–3). This error occurred to a lesser extent in simulation scheme 3, since in the LRDEM the channel was completely 'smoothed-out'. Consequently, a more uniform distribution of rock impacts was produced.

The squares with an overestimation of 10.7% and an underestimation of 7.9% in figure 8 (scheme 1) indicate a spatial mismatch between model results and field observations. Figure 8 shows that simulation schemes 2 and 3 have an underestimation only in the same area, which is about 12%. The errors in the validation squares on the lowest part of the test site show that the simulation schemes 1–3 modelled the maximum extent of rockfall runout zones quite well (figure 5), as the error values in those parts are smaller than 5%. None of the simulation schemes produced rocks at the bottom part of the hill slope, which is in agreement with reality. As mentioned before, the modelled rockfall impacts on tree stems reproduced the trend observed in reality, but were not very accurate as the MSEs of all the simulation schemes were quite high.

5.3. *Rockfall simulation at different scales*

Overall, the results indicate that the GIS-based distributed model used in this study, which was developed for rockfall assessment at a slope scale, can be used for rockfall assessment at a regional scale. As expected, the simulation schemes analysed indicated that input data with a support of 25×25 m increased the MSE

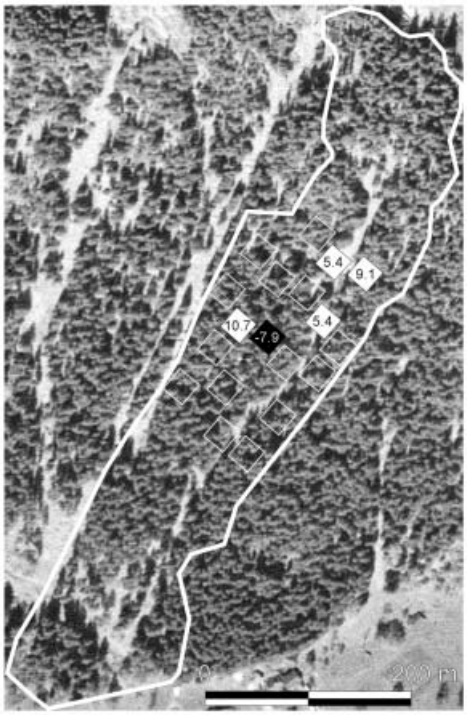

SCHEME 1

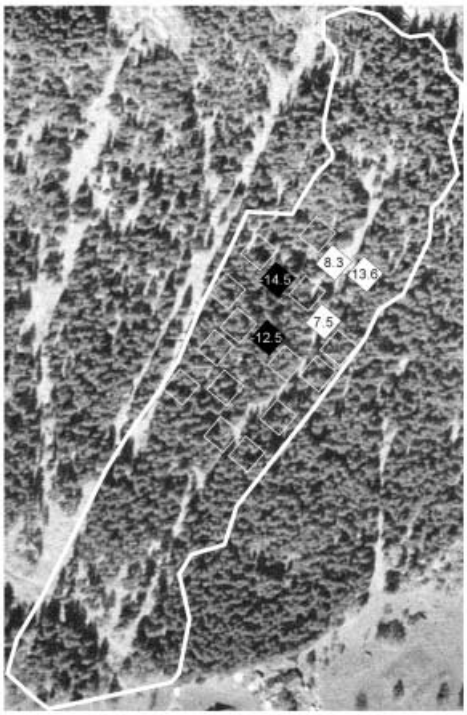

SCHEME 2

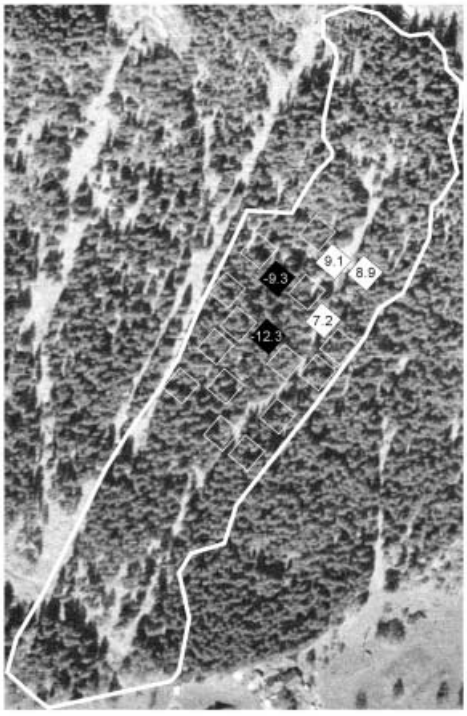

SCHEME 3

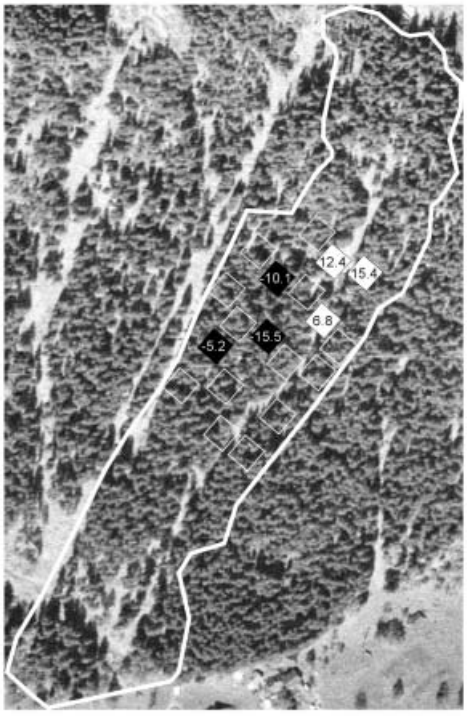

SCHEME 4

compared to input data with a support of 2.5×2.5 m. However, the simulated maximum extents of rockfall runout zones were similar for simulation schemes 1–3. In addition, these simulated maxima also corresponded with those observed in reality, which shows that modelling rockfall runout zones at the regional scale is feasible and realistic, even for forested catchments. The simulated rockfall impacts on tree stems using data with a support of 25×25 m were not accurate, as the mean-squared errors produced by simulation schemes 2 and 3 were much larger than the MSE of scheme 1. Using tree distribution data of higher quality could reduce the MSE of scheme 3 with about 2% as shown by the 'intermediate' simulation scheme 7. The accuracies of the results produced by schemes 2 and 3 indicate that simulating damage on tree stems caused by rockfall using data with a support of 25×25 m is not realistic. To assess where and how much tree stem damage will occur, high quality data with a small support are required.

6. Conclusions

This paper has investigated the relationship between the aggregation level of the input data and the accuracy of the output of a rockfall simulation model. The results showed that the simulation of rockfall with a GIS-based distributed model using data with a support of 25×25 m is feasible and realistic to simulate rockfall runout zones, but not for the simulation of tree damage caused by rockfall. The latter arose because collisions of rocks against tree stems cannot be simulated accurately where the data are of poor quality and the support is large.

As anticipated, the model using data with a support of 25×25 m produces a larger error than that using data with a support of 2.5×2.5 m. Our hypothesis was that poor data quality is a more important cause of a larger model prediction error than the effect of a larger support. This study showed that this is not necessarily true because the simulation scheme that used data of higher quality produced a larger error than the simulation scheme that used data of poorer quality. Here it was interesting to observe that the loss of important spatial structure in the input data (i.e. the rockfall channel represented in the slope map and in the tree distribution map), as caused by spatial aggregation, resulted in a larger model prediction error than the use of data that represented the landscape with less detail.

The results of this study also indicate that the use of a regional DEM of high quality requires data on forest structure of higher quality than does a regional DEM of poorer quality in case of simulating rocks falling through mountain forests. We realize that other spatial simulation models and other input data than those used in this study may well produce quite different results. However, since the forest that was chosen as a study area is representative for many forests that protect houses and infrastructure in the European Alps, we consider the outcomes also applicable for other forests in the European Alps. The main reason for this is that steep non-forested tracks, which are often preferential rockfall and also avalanche tracks, occur in many of these protection forests. The existence of such non-forested tracks was the main reason why the simulation scheme that used a DEM and tree

Figure 8. Visualization of the validation squares, where $|P_i - O_i| > 5$ for simulation schemes 1–3 as well as 'intermediate' scheme 4. The white outlined squares indicate an absolute error smaller than 5; black filled squares indicate significant underestimation by the model; white filled squares indicate significant overestimation by the model.

structure data at different supports was the most inaccurate. The same effect is likely to happen when using data from other rockfall forests. It would be interesting to aim future rockfall modelling research determining the minimum support required to obtain realistic and trustworthy modelling results for the assessment of the degree of protection provided by mountain forests against rockfall hazards in the European Alps. These assessments probably could be done using data with a support ranging from 1 to 25 m, but the question is which support would be sufficient. Goodchild (2001) stated that the input data for a model should be of sufficient detail to capture the spatial variation that is essential to describe the process or pattern being modelled. The results of this study confirm this, because it shows that to model tree damage caused by rockfall, the tree distribution must be known at a level of detail that corresponds with the physical process of rockfall.

References

AZZONI, A., BARBERA, G. L., and ZANINETTI, A., 1995, Analysis and prediction of rockfalls using a mathematical model. *International Journal of Rock Mechanics and Mining Science*, **32**, 709–724.

BERGKAMP, G., 1995, A hierarchical approach for desertification assessment. *Environmental Monitoring and Assessment*, **37**, 1–20.

BEV, 2002, Bundesamt für Eich- und Vermessungswesen, Produktinformation zum Geländehöhenmodell (available at: http://www.bev.gv.at/prodinfo/dgm/dgm_3f.htm).

BIERKENS, M. F. P., FINKE, P. A., and DE WILLIGEN, P., 2000, *Upscaling and Downscaling Methods for Environmental Research* (Dordrecht: Kluwer).

BITTERLICH, W., 1948, Die Winkelzählprobe. *Allgemeine Forst und Holzwirtschaftliche Zeitung*, **1**, 4–5.

BURROUGH, P. A., and MCDONNELL, R. A., 1998, *Principles of Geographical Information Systems* (Oxford: Oxford University Press).

CHAU, K. T., WONG, R. H. C., and LEE, C. F., 1998, Rockfall problems in Hong Kong and some new experimental results for coefficient of restitution. *International Journal of Rock Mechanics and Mining Science*, **35**, 662–663.

CHAU, K. T., WONG, R. H. C., and WU, J. J., 2002, Coefficient of restitution and rotational motions of rockfall impacts. *International Journal of Rock Mechanics and Mining Science*, **39**, 69–77.

DORREN, L. K. A., MAIER, B., PUTTERS, U. S., and SEIJMONSBERGEN, A. C., 2004, Combining field and modelling techniques to assess rockfall dynamics on a protection forest hillslope in the European Alps. *Geomorphology*, **57**, 151–167.

DORREN, L. K. A., and SEIJMONSBERGEN, A. C., 2003, Comparison of three GIS-based models for predicting rockfall runout zones at a regional scale. *Geomorphology*, **56**, 49–64.

GIANI, G. P., 1992, *Rock Slope Stability Analysis* (Rotterdam: Balkema).

GOODCHILD, M. F., 2001, Models of scale and scales of modeling. In *Modelling Scale in Geographical Information Systems*, edited by N. J. Tate and P. M. Atkinson (Chichester: Wiley), pp. 3–10.

HEUVELINK, G. B. M., 1998, Uncertainty analysis in environmental modelling under a change of spatial scale. *Nutrient Cycling in Agroecosystems*, **50**, 255–264.

KOBAYASHI, Y., HARP, E. L., and KAGAWA, T., 1990, Simulation of rockfalls triggered by earthquakes. *Rock Mechanics and Rock Engineering*, **23**, 1–20.

LEWIS, P. A. W., and ORAV, E. J., 1989, *Simulation Methodology for Statisticians, Operations Analysts, and Engineers*, Vol. 1 (Pacific Grove: Wadsworth & Brooks/Cole).

MAIER, B., 1993, Forstinventur Stand Montafon. Internal Report (Schruns, Austria: Stand Montafon).

MEIßL, G., 1998, Modellierung der Reichweite von Felsstürzen. Fallbeispeile zur GIS-gestützten Gefahrenbeurteilung aus dem Beierischen und Tiroler Alpenraum. PhD thesis, Universität Innsbruck.

MONTGOMERY, D. R., and DIETRICH, W. E., 1994, A physically-based model for the

topographic control on shallow landsliding. *Water Resources Research*, **30**, 1153–1171.

MOWRER, H. T., 1997, Propagating uncertainty through spatial estimation processes for old-growth subalpine forests using sequential Gaussian simulation in GIS. *Ecological Modelling*, **98**, 73–86.

PFEIFFER, T. J., and BOWEN, T. D., 1989, Computer simulation of rockfalls. *Bulletin of the Association of Engineering Geologists*, **26**, 135–146.

QUINN, P., BEVEN, K., CHEVALLIER, P., and PLANCHON, O., 1991, The prediction of hillslope flow paths for distributed hydrological modelling using digital terrain models. *Hydrological Processes*, **5**, 59–79.

SHIVER, B. D., and BORDERS, B. E., 1995, *Sampling Techniques for Forest Resource Inventory* (New York: Wiley).

TARBOTON, D. G., 1997, A new method for the determination of flow directions and contributing areas in grid digital elevation models. *Water Resources Research*, **33**, 309–319.

TUCKER, G. E., LANCASTER, S. T., GASPARINI, N. M., BRAS, R. L., and RYBARCZYK, S. M., 2001, An object-oriented framework for distributed hydrologic and geomorphic modeling using triangulated irregular networks. *Computers and Geosciences*, **27**, 959–973.

VAN DIJKE, J. J., and VAN WESTEN, C. J., 1990, Rockfall hazard: a geomorphological application of neighbourhood analysis with ILWIS. *ITC Journal*, **1**, 40–44.

VAN ROMPAEY, A., GOVERS, G., and BAUDET, M., 1999, A strategy for controlling error of distributed environmental models by aggregation. *International Journal of Geographical Information Science*, **13**, 577–590.

WILLGOOSE, G. R., BRAS, R. L., and RODRIGUEZ-ITURBE, I., 1991, A physically based coupled network growth and hillslope evolution model, 1, theory. *Water Resources Research*, **27**, 1671–1684.

WOLOCK, D. M., and MCCABE, G. J., JR, 1995, Comparison of single and multiple flow direction algorithms for computing topographic parameters in TOPMODEL. *Water Resources Research*, **31**, 1315–1324.

ZEVENBERGEN, L. W., and THORNE, C. R., 1987, Quantitative analysis of land surface topography. *Earth Surface Processes and Landforms*, **12**, 47–56.